IOPscience iopscience.iop.org

Home Search Collections Journals About Contact us My IOPscience

Structural and optical properties of Yb-implanted silicon

This article has been downloaded from IOPscience. Please scroll down to see the full text article.

1995 J. Phys.: Condens. Matter 7 2533

(http://iopscience.iop.org/0953-8984/7/13/004)

View the table of contents for this issue, or go to the journal homepage for more

Download details:
IP Address: 171.66.16.179
The article was downloaded on 13/05/2010 at 12:50

Please note that terms and conditions apply.

J. Phys.: Condens. Matter 7 (1995) 2533–2540. Printed in the UK

Structural and optical properties of Yb-implanted silicon

Li Dai-qing†, Ren Ting-qi†, Wan Ya†, Chen Hong‡, Zhu Pei-ran‡ and Xu Tian-bing‡

† Department of Physics, Yantai Teachers' University, Yantai 264025, People's Republic of China

‡ Institute of Physics, Chinese Academy of Sciences, Beijing 100080, People's Republic of China

Received 7 November 1994

Abstract. TEM and PL combined with the RBS technique have been used to investigate the rapid-thermal-annealing-induced structural and optical properties of Yb-implanted silicon. For anneals at 800, 900 and 1000 °C, the initial recrystallization of the amorphous layer is epitaxial, followed by a disruption of the regrowth with the remaining damaged region rich in planar defects with plenty of precipitates observed in the recrystallized region. In the same annealing regime, the best crystal quality and highest intensity of PL are observed for the sample annealed at 1000 °C. During annealing, Yb segregates not only at the crystal–amorphous interface but also at the surface at the same time. For the anneal at 1200 °C, however, almost all the Yb has piled up at the surface, which leads to the disappearance of the PL although the amorphous layer has regrown completely with an excellent crystal quality. It is proposed that both the amount of Yb incorporated into the epitaxially recrystallized region and its crystal quality are responsible for the efficiency of optical activation.

1. Introduction

The incorporation of rare-earth (RE) elements into semiconductors is attracting much interest. Because the incompletely filled 4f shells of RE elements are effectively screened by the outer 5p and 6s electrons, their luminescence is sharp and almost temperature independent. This may allow the synthesis of useful luminescing materials. Work has been focused on RE-implanted Si to make optoelectronic devices. Unfortunately, because of the unmatched atomic radius between Si and RE elements, the solubility of RE elements in Si is quite low and the equilibrium processing method, therefore, cannot be used for this. As a non-equilibrium processing method, ion implantation combined with thermal annealing has been demonstrated to be effective in increasing the concentration of RE elements incorporated into silicon [1–7]. Recently, using the ion implantation method, we have incorporated both Er and Yb into silicon up to 10^{20} cm^{-3} [8, 9]. In this study, we shall discuss rapid-thermal-annealing- (RTA-) induced recrystallization, microstructure, redistribution of the impurities and its optical activation in Yb-implanted silicon.

2. Experimental details

Czochralski-grown P-type Si(100) wafers with a resistivity of about 10 Ω cm were used in the experiment. The 350 keV Yb^+ ions were implanted into Si(100) with the samples at room temperature to a dose of 1×10^{15} cm^{-2}. The samples were tilted 7° off the

0953-8984/95/132533+08$19.50 © 1995 IOP Publishing Ltd

incident ion beam in order to prevent channelling effects. Following implantation, RTA was carried out at 800, 900, 1000 and 1200 °C in a dry nitrogen atmosphere. For a more detailed observation of the changes in the microstructure and their correlation with the photoluminescence (PL), a relatively short period of RTA, 5 s, is chosen. Cross-sectional transmission electron microscopy (TEM) was used to characterize the residual damage and the formation of precipitates in the annealed samples. Rutherford backscattering spectrometry (RBS) and ion channelling using 4.2 MeV Li^{2+} as the analysing beam were used to determine the amount of damage and the depth profile of implanted Yb for both as-implanted and annealed samples. The backscattered particles were detected at an angle of 165°. The combination of TEM and RBS can give us more complete information about the factors which influence the changes in the microstructure and the PL intensity. PL spectra were measured at 77 K to monitor the changes in the optical activation of Yb after RTA at different temperatures. The 488 nm line of an Ar^+ laser was used as a pump source and the PL spectra were detected using a monochromator and a liquid-nitrogen-cooled germanium detector.

3. Experimental results

3.1. Transmission electron microscopy observation

Figure 1 shows cross-sectional TEM photographs of Yb^+-implanted samples after RTA at 800, 900, 1000 and 1200 °C. In sample a, which was annealed at 800 °C, two obviously different regions are observed. Region I is from the surface to 175 nm, while region II extends from 175 nm to the end of the range (EOR), 330 nm. In region II, a high density of small precipitates have a random distribution. Region I, in fact, is a residually damaged region in which many stacking faults and microtwins are observed and the crystal quality suddenly deteriorates. For sample b annealed at 900 °C, three different regions are observed. Region I, which is from the surface to 160 nm, is a little thinner and the size of stacking faults and microtwins in it are larger than those for the sample annealed at 800 °C. Also, the density of defects in region I is greatly reduced. In region II from 160 to 260 nm, a high crystal quality is observed, in which there are almost no precipitates and stacking faults. At the depth of EOR is region III which has a width of about 70 nm and is full of large precipitates. It should be noted that the precipitates in region III grow larger and their density is also lower than for the sample annealed at 800 °C. For the sample annealed at 1000 °C, the microstructure is similar to that for the sample annealed at 900 °C. However, both the size of precipitates in region III and the size of stacking faults and microtwins in region I are larger than for samples a and b in the corresponding areas. It should also be noted that there is a layer of precipitates at the crystal–amorphous interface for samples a, b and c. Also, the boundary between region I and region II is clearly distinguished in samples a and b. Nevertheless, there is no obvious boundary between region I and region II in sample c owing to the better regrowth. The crystal quality in sample c as a whole is better than that in sample a and sample b. For sample d annealed at 1200 °C, the crystal quality has made an excellent recovery after RTA. The residual damage of precipitates and planar defects can only be observed at the surface, which are rather dilute and large.

3.2. Rutherford backscattering spectrometry and photoluminescence

Shown in figure 2 are aligned and random spectra of the silicon signal before and after RTA at 800, 900, 1000 and 1200 °C for 5 s. As-implanted samples were amorphized to the

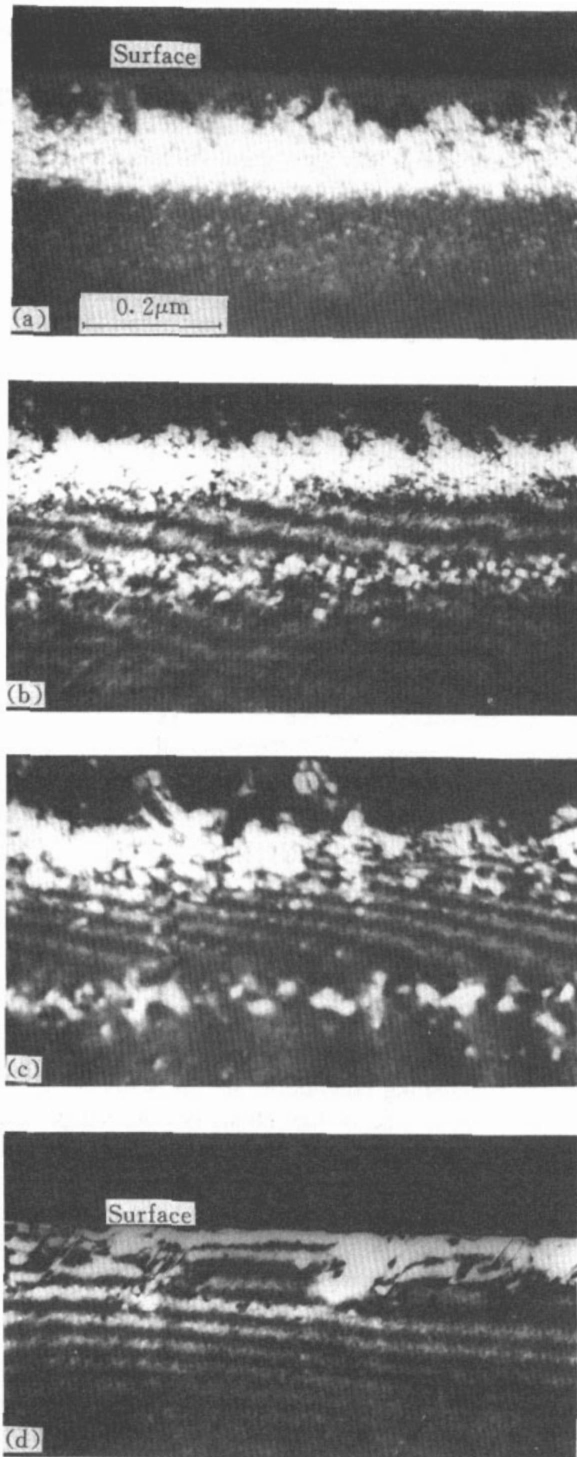

Figure 1. Cross-sectional transmission electron micrographs of Yb-implanted silicon after RTA at (*a*) 800 °C, (*b*) 900 °C, (*c*) 1000 °C and (*d*) 1200 °C.

depth of about 300 nm. During the anneals at 800, 900 and 1000 °C, the initial regrowth is epitaxial, but the remaining damaged region is polycrystalline with a poor crystal quality. The anneals at 800, 900 and 1000 °C reduce the width of the amorphous layer to 123 nm, 105 nm and 94 nm, respectively. However, the anneal at 1200 °C for 5 s caused the amorphous layer to regrow completely, leaving a small damage peak at the surface. The RBS and TEM observations are basically in agreement.

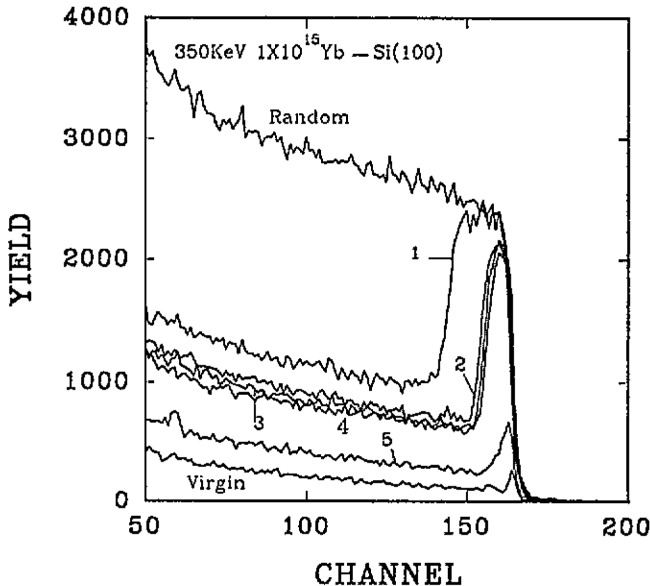

Figure 2. The silicon portions of the spectra obtained by RBS and channelling for 1×10^{15} cm^{-2} 350 keV Yb^{+}-implanted samples as-implanted (curve 1), and following RTA at 800 °C (curve 2), 900 °C (curve 3), 1000 °C (curve 4) and 1200 °C (curve 5).

Figure 3 shows Yb portions of the RBS random spectra for 350 keV Yb^{+}-implanted samples both as-implanted and annealed at different temperatures. The Yb profiles are identical under random and channelling conditions; so Yb is not on substitutional lattice sites. For clarity, the channelling spectra of the Yb signals are not presented in figure 3. After the RTA at 800, 900 and 1000 °C, the Yb segregates not only at the crystalline–amorphous interface but also at the surface at the same time, which is different from the usual segregation of the Er only at the crystalline–amorphous interface for Er-implanted silicon [2, 11]. In addition, the extent of segregation of Yb at the crystalline–amorphous interface decreases with increasing annealing temperature, while the extent at the surface increases with the increase in annealing temperature. After annealing at 1200 °C, however, in addition to the complete recrystallization of the amorphous layer, almost all the Yb has piled up at the surface.

The Yb-related PL at 77 K is shown in figure 4. The intensity of the PL also has a strong dependence on the annealing temperature. For the as-implanted sample, no PL peak is observed in the detection limit of the spectrometer. Following the anneal at 800 °C, the PL peaks appear with the main peak centred at about 1 μm. At the same time, a weak line is also observed on the longer-wavelength side. Upon further increase in the annealing temperature to 900 °C, the intensity of the main peak has a slight increase. The

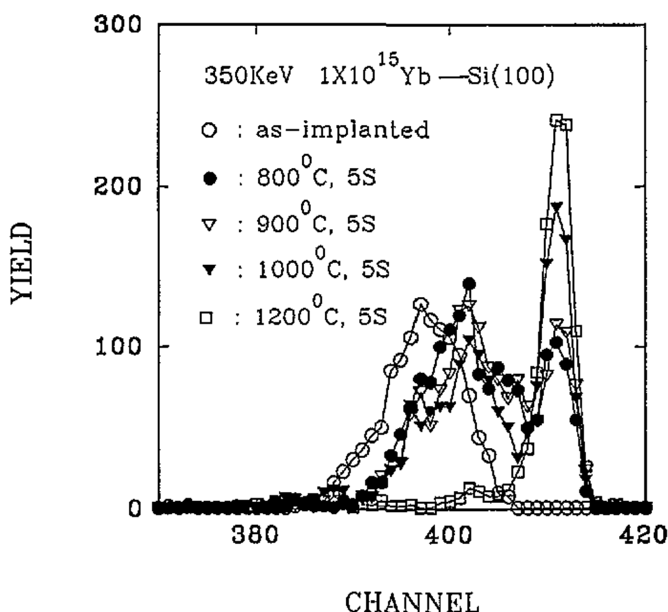

Figure 3. The Yb portions of spectra obtained by RBS for the samples as-implanted and after RTA at 800 °C, 900 °C, 1000 °C and 1200 °C.

strongest emission at about 1 μm is observed after the anneal at 1000 °C, but the sample annealed at 1200 °C does not luminesce at all. The enhancement and annihilation of the Yb-related luminescence are closely related to the migration of the Yb during RTA and to the microstructure in the recrystallized region. We shall discuss this relationship later.

4. Discussion

During the anneals at 800, 900 and 1000 °C, the crystalline–amorphous interface sweeps through the as-implanted Yb profile. Meanwhile most of the Yb segregates at the crystalline–amorphous interface and migrates towards the surface with the moving crystalline–amorphous interface. When the epitaxial growth is disrupted, the peak of Yb almost coincides with the crystalline–amorphous interface. From the calculation based on figures 2 and 3, the Yb concentrations at the peak of the Yb profile are as high as 1.27×10^{20} cm^{-3}, 1.15×10^{20} cm^{-3} and 0.95×10^{20} cm^{-3}, following the RTA at 800 °C, 900 °C and 1000 °C, respectively. This indicates that the high concentration of Yb at the crystalline–amorphous interface is at least partially responsible for the disruption of the regrowth. In figures 1(b) and 1(c), the precipitates are mainly concentrated at the EOR and crystalline–amorphous interface. Meanwhile, there are almost no precipitates in region II which is between the EOR and crystalline–amorphous interface. It seems that during the anneal the Yb tends to be pushed out of the recrystallized region which has a high crystal quality. In fact, the highly effective region at the crystalline–amorphous interface will supply plenty of gettering sites for Yb and as a result much of the Yb will segregate at the crystalline–amorphous interface. Because the trapping of the Yb in the crystal silicon is limited by the low solubility, some of the Yb in the recrystallized region near the crystalline–amorphous interface will aggregate to form precipitates which can be seen in figures 1(a)–(c). In addition, it is common knowledge

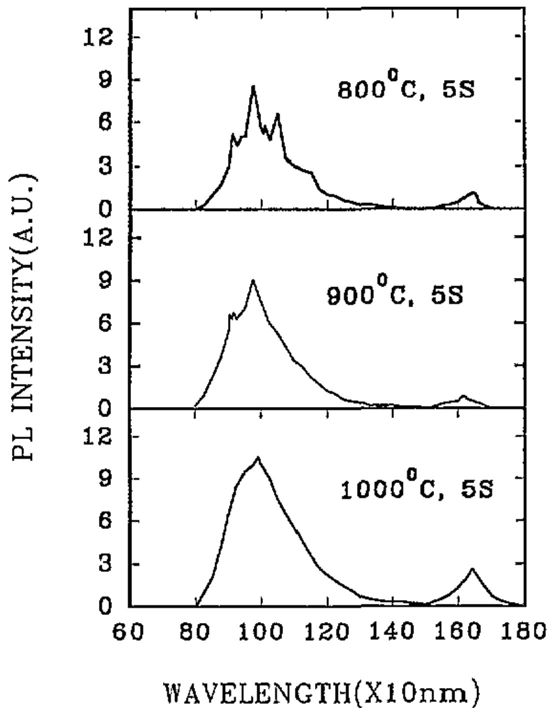

Figure 4. PL spectra for Yb^+-implanted silicon at 77 K after RTA at 800, 900 and 1000 °C (A.U., arbitrary units).

that the secondary defects usually form at the depth of the EOR after the regrowth of an amorphous layer [10]. The secondary defects at the EOR act as gettering sites for Yb and the precipitates are thus formed at the EOR. We may conclude that the precipitates tend to be formed at a boundary between a defective region and a region with high crystal quality. As an exception, the random distribution of precipitates in the recrystallized region for the sample annealed at 800 °C is related to the poor crystal quality in it.

A recent study by Polman *et al* [11] demonstrated that the epitaxial growth of the amorphous layer caused by Er implantation is disrupted once a fixed Er concentration is reached at the crystalline–amorphous interface and, when the epitaxy is disrupted, an Er segregation spike will appear at the region near the crystalline–amorphous interface. Accompanied by the movement of the crystalline–amorphous interface towards the surface, the Er segregation spike also moves with it. This is quite similar to our result. The only difference is that Yb seems more difficult to trap in the crystal. In addition to segregation at the crystalline–amorphous interface, Yb also segregates at the surface at the same time, which is different from the usual segregation of Er at the crystalline–amorphous interface. The difference between the atomic radii of Yb and Er (0.194 nm and 0.176 nm, respectively) may be responsible for their different segregation behaviours. Even though the Yb remains non-substitutional, its large atomic radius (compared with silicon, 0.118 nm) will generate a large lattice strain which makes it more energetically unfavourable for it to be trapped in a perfect crystal lattice or even to stay in the remaining damaged region than is the case for Er. Therefore, in addition to the Yb segregation at the crystalline–amorphous interface, which is similar to the Er segregation, Yb also has a strong tendency to segregate at the surface simultaneously. Because the migration of Yb towards the surface is enhanced by

the thermodynamic energy, the extent of the Yb segregation at the surface increases with an increase in annealing temperature. The thermodynamic energy for the RTA at 1200 °C is high enough to inhibit the formation of precipitates and impurity–defect complexes. The migration of the Yb towards the surface is thus much enhanced so that most of it piles up at the surface after annealing.

TEM combined with RBS measurements reveal that there are two different temperature regimes for the regrowth of the amorphous layer and the migration of the Yb. A critical temperature higher than 1000 °C and lower than 1200 °C may exist, above which both the regrowth rate and the extent of the Yb migration towards the surface are greatly enhanced. For the anneals at 800, 900 and 1000 °C, further regrowth of the remaining damaged region is prohibited by the precipitates formed at the crystalline–amorphous interface and the high density of planar defects which bind Yb atoms at them to form impurity–defect complexes. During the anneal at 1200 °C, the migration of the Yb towards the surface is enhanced to such an extent that almost all the Yb has piled up at the surface and at the same time the thermodynamic energy is also high enough to decompose most of the planar defects. Therefore, the amorphous layer regrows completely. After the discussion of structural properties and migration of the Yb during the anneal, we can better understand the mechanism of the optical activation. For the as-implanted sample, the amorphous environment for Yb completely suppresses its optical activation. After RTA at 800 °C, the epitaxial regrowth of the amorphous layer and the improvement in the crystal quality in the remaining damaged region causes some of the Yb to be optically activated. In the annealing regime from 800 to 1000 °C, even though the concentration of the Yb in the recrystallized region and the area near the crystalline–amorphous interface decreases with increasing annealing temperature, the intensity of the PL increases with increasing annealing temperature. At the same time, the higher annealing temperature corresponds to a better crystal quality. We may thus conclude that both the amount of the Yb incorporated into the epitaxially recrystallized region and its crystal quality are responsible for the efficiency of optical activation. For the anneal at 1200 °C, almost all the Yb has piled up at the surface. This leads to complete annihilation of the PL although the recrystallized region has the best crystal quality. It should be noted that, during annealing, competition exists between the incorporation of the Yb into the recrystallized region and the improvement in crystal quality. When the annealing time and the annealing method are fixed, a higher annealing temperature usually corresponds to a better crystal quality, whereas the amount of the Yb incorporated in the recrystallized region decreases with increasing annealing temperature, which results from the limited solid solubility of the Yb in silicon. It is possible to determine the optimum annealing condition for the highest optical activation from more detailed choices of the annealing time and temperature.

5. Conclusion

In summary, cross-sectional TEM, RBS, ion channelling and PL have been used to investigate the structural and optical properties of Yb-implanted silicon. Two annealing regimes are observed. In the annealing regime from 800 to 1000 °C, the amorphous layer initially regrows epitaxially, followed by disruption of the regrowth. It is also observed that a higher annealing temperature corresponds to a better crystal quality in the recrystallized region and the remaining damaged region. Meanwhile, Yb segregates not only at the crystalline–amorphous interface but also at the surface, which is different from the usual crystalline–amorphous interfacial segregation of the Er. As for the optical activation, the

intensity of the PL increases with increasing annealing temperature in the same annealing regime. For RTA at 1200 °C, accompanied by the complete regrowth of the amorphous layer, almost all the Yb has piled up at the surface, which is responsible for the annihilation of the Yb luminescence. The microstructure and the redistribution of Yb after annealing indicate that the amount of the Yb incorporated into the recrystallized region and its crystal quality are responsible for the efficiency of optical activation and there is competition between the improvement in crystal quality and the amount of the Yb incorporated into the recrystallized region. Further investigation is needed to optimize the experimental conditions and to clarify the mechanism of the relevant processes.

Acknowledgments

This work is partly supported by the Foundation of the Educational Committee of Shandong Province. We would like to acknowledge H Y Lu for her contributions to this work.

References

[1] Tsang W J and Logan R A 1986 *Appl. Phys. Lett.* **49** 1686
[2] Zhang J P, Tang Y S, Hemment P L F and Sealy B J 1990 *Nucl. Instrum. Methods* B **47** 155
[3] Gillin W P, Zhang J P and Sealy B J 1991 *Solid State Commun.* **77** 907
[4] Kozanecki A and Groetzschel R 1990 *J. Appl. Phys.* **68** 517
[5] Lombardo S, Campisano S U, van den Hoven G N, Cacciato A and Polman A 1993 *Appl. Phys. Lett.* **63** 1942
[6] Fleuster M, Buchal Ch, Snoeks E and Polman A 1994 *J. Appl. Phys.* **75** 173
[7] Custer J S, Polman A and van Pinxteren H M 1994 *J. Appl. Phys.* **75** 2809
[8] Xu T B, Zhu P R, Li D Q, Ren T Q, Sun H L and Wan S K 1994 *Phys. Lett.* **189A** 423
[9] Li D Q, Ren T Q, Gong B A, Zhang B, Chen K J, Zhu P R and Xu T B 1994 *Mater. Sci. Eng.* B at press
[10] Jones K S, Prussin S and Weber E R 1988 *Appl. Phys.* A **45** 1
[11] Polman A, Custer J S, Snoeks E and van den Hoven G N 1993 *Appl. Phys. Lett.* **62** 507